Precise determination of object position in 1D optical lattice

Tomáš Čižmár, Martin Šiler, Mojmír Šerý and Pavel Zemánek

Institute of Scientific Instruments, Academy of Sciences of the Czech Republic,
Královopolská 147, 612 64 Brno, Czech Republic

ABSTRACT

We present a new and precise method how to employ a periodic interference illumination for axial particle position determination. Particle movement with respect to the interference structure of illumination is followed by changes in the light field scattered by the particle. Analyses of these changes together with their calibration provide an excellent way how to determine not only the particle position with respect to the camera but especially with respect to the illuminating field structure. The algorithm was used in a standing wave optical trap for determination of the trap properties and particle behavior even in the standing wave in motion.

Keywords: optical trapping, particle tracking, colloidal particle

1. INTRODUCTION

The particle tracking is nowadays very important tool to study elementary processes at the molecular level,[1–7] to perform a variety of colloidal studies,[8–11]to visualize fluid dynamics and to study Brownian motion and diffusion under various conditions leading to rectification of the particle motion.[12,13] Even molecular orientation can be detected by an optical means from the CCD image analyses.[14] Usually fluorescent objects are detected by sensitive CCD camera in two dimensions because they can be tracked in complex environment. Different algorithms are used to extract the object position in nanometer resolution.[15,16] This CCD based technique was extended to 3D by adding the axial direction using off-focus imaging.[17,18] Other methods are especially connected with optical tweezers and use quadrant photodiode to detect either the object lateral motion[19,20] or even 3D motion of single microobject with subnanometer spatial resolution and microsecond temporal resolution.[21–25] The most precise method is based on the polarization changes of the light measured by a pair of detectors.[26] This method measures picometer displacements of transparent microscopic object but only in one direction. Unfortunately these methods using photodiodes can follow only single object. Novotny et. al used CCD to detect the fluorescence from single molecules illuminated by a radially polarized beam and from the fluorescence image they were able to determine the orientation of the absorption dipole of the molecules.[14,27]

Recently analyses of the particle motion near an interface attracted a great attention especially in connection with the evanescent wave illumination. A new microscopic method have been developed – total internal reflection microscopy[28,29] – that employs the exponential decay of the illuminating field with the increasing distance from the surface. Therefore the intensity decay of the detected scattered field or fluorescence signal is used to obtain the distance of the object from the surface.[30,31]

Here we present a method that uses a CCD to detect the field scattered by an object perpendicularly to the direction of illuminating beam. The novelty of this methods is based on the spatially periodic illuminating field - for example a standing wave or more complicated interference pattern. If the size of the object is comparable and bigger than spatial period of the field, the shape of the scattered image is very sensitive to the location of the object with respect to the intensity maxima and minima of the illuminating beam. This principle can be extended into two dimensions if a sort of two dimensional spatially periodic pattern in used.

The new method is a product of our research on particle behavior in the standing wave.[32–34] The standing wave - interference field of two counterpropagating beams - can serve as a periodic system of optical traps for particle confinement and controllable delivery. The position of the standing wave structure (nodes and antinodes) is set by the phase difference between the interfering beams. Therefore altering phase in one beam causes the motion of the standing wave together with the confined particles (the optical conveyor belt).[32]

Further author information: (Send correspondence to P.Z.)
P.Z.: E-mail: pavlik@isibrno.cz, Telephone: +420 541 514 202, Fax: +420 541 514 402

Optical Trapping and Optical Micromanipulation III, edited by Kishan Dholakia, Gabriel C. Spalding,
Proc. of SPIE Vol. 6326, 632627, (2006) · 0277-786X/06/$15 · doi: 10.1117/12.680563

2. THEORETICAL DESCRIPTION OF THE INTERFERENCE PATTERN FORMED BY THE SCATTERED LIGHT

For the detailed quantitative investigation of the parameters of the optical traps (depths of the potential well, optical stiffnesses) we needed to track the particle position precisely. Therefore we used the light of the trapping field scattered by the particle. The scattered light was imaged by a microscope objective into the plane of CCD camera. In this plane the imaged light forms an intensity pattern with a specific shape. Applying the particle tracking algorithms which are routinely used in cases of single beam illumination[15] to our record of scattered intensity patterns we obtained particle-position data inconsistent with the possible particle behavior in such potential energy landscape. The processed data indicated that the particle displacement from the stable position were larger than the extent of the optical trap. These errors were caused due to the fact that the intensity pattern of the light scattered by the particle does not keep the same shape while the particle moves in the illuminating standing wave (see Fig. 2).

To overcome this effect we could use other single beam illumination on a different wavelength and filter out the scattered light of the trapping field. However, this would be an enormous wasting of valuable information, because the shape of the intensity pattern carries the information about the particle position with respect to the periodic illuminating field.

Let us assume that a scatterer (particle) stays static in the laboratory system of Cartesian coordinates $\bar{x}$, $\bar{y}$, $\bar{z}$ (optical system and CCD) as Fig. 1 demonstrates (the accents $^-$ are used to distinguish the Cartesian coordinates $\bar{x}, \bar{y}, \bar{z}$ from the particle position x, y, z). Let us illuminate the particle by a standing wave moving in the direction of $\bar{z}$ axis (since the standing wave is the result of interference of two counter-propagating waves, the motion of the standing wave is controlled by changing the phase of one of these interfering waves). The scattered light is imaged on the plane of CCD camera. For the following description the scalar concept of electromagnetic

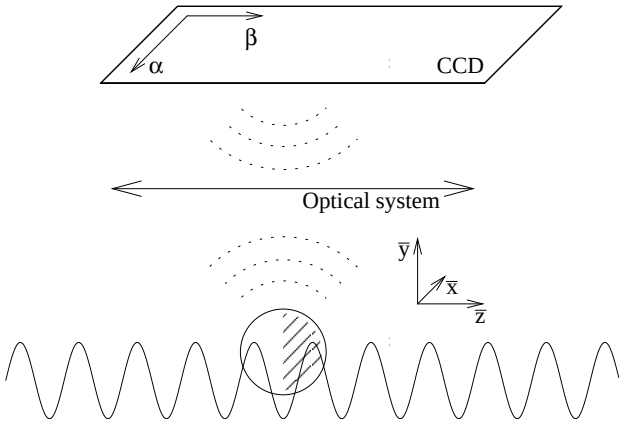

Figure 1. The conception of fixed particle (scatterer) in the movable standing wave

field is used. If we considered the vectorial description, it would give the same result as the scalar one, however it would make the description much more complicated.

The scatterer is surrounded by the electric field $E(\bar{x}, \bar{y}, \bar{z}, t)$ of the moving standing wave. The scattered light creates an electromagnetic field $E_{CCD}(\alpha, \beta, t)$ in the plane of the CCD. E and E_{CCD} are linked by a impulse response function $f(\bar{x}, \bar{y}, \bar{z}, \alpha, \beta)$ of the imaging system and the particle. This function denotes how the unity volume of the particle submerged into the field E at $\bar{x}, \bar{y}, \bar{z}$ forms the field E_{CCD} at the position of α, β in the CCD plane. Since no nonlinearities of all media (on the way of the scattered field to the CCD) are assumed the relationship between E and E_{CCD} can be written in the following form:

$$dE_{CCD}(\alpha, \beta, t) = f(\bar{x}, \bar{y}, \bar{z}, \alpha, \beta) \cdot E(\bar{x}, \bar{y}, \bar{z}, t)\ d\bar{x}\ d\bar{y}\ d\bar{z}. \tag{1}$$

In the most general case, the moving standing wave (conveyor belt) can be described as two counter-propagating beams with alterable phase of one of them. To simplify the explanation but to keep the key features we assume that the complex amplitudes of these beams are $\bar{z}$-independent. This conception is valid for the plane wave, the non-diffracting beams or the evanescent wave, and can be used for approximative description of real spatially limited beams assuming the geometrical optics approximation. The motional standing wave has the form:

$$\begin{aligned} E(\bar{x},\bar{y},\bar{z},t) &= E_1(\bar{x},\bar{y})e^{i(k\bar{z}-\omega t)} + E_2(\bar{x},\bar{y})e^{i(-k(\bar{z}-2z_\psi)-\omega t)} \\ &= e^{-i\omega t}\left[E_1(\bar{x},\bar{y})e^{ik\bar{z}} + e^{2ikz_\psi}E_2(\bar{x},\bar{y})e^{-ik\bar{z}}\right], \end{aligned} \tag{2}$$

where $E_1(\bar{x},\bar{y})$ and $E_2(\bar{x},\bar{y})$ are the complex amplitudes of the electric field and z_ψ is the position of the standing wave structure. Changing the value of z_ψ (altering the phase difference by changing the length of path of one beam) causes the movement of the nodes and antinodes of the standing wave. The total field in the plane of CCD can be expressed using Eqs. (1) and (2):

$$\begin{aligned} E_{CCD}(\alpha,\beta,t) &= \oint_{scatterer} f(\bar{x},\bar{y},\bar{z},\alpha,\beta)\cdot E(\bar{x},\bar{y},\bar{z},t)\; d\bar{x}\; d\bar{y}\; d\bar{z} \\ &= e^{-i\omega t}\left[\oint_{scatterer} f(\bar{x},\bar{y},\bar{z},\alpha,\beta)\cdot E_1(\bar{x},\bar{y})e^{ik\bar{z}}\; d\bar{x}\; d\bar{y}\; d\bar{z}\right. \\ &+ \left. e^{2ikz_\psi}\oint_{scatterer} f(\bar{x},\bar{y},\bar{z},\alpha,\beta)\cdot E_2(\bar{x},\bar{y})e^{-ik\bar{z}}\; d\bar{x}\; d\bar{y}\; d\bar{z}\right]. \end{aligned} \tag{3}$$

Even-though the function $f(\bar{x},\bar{y},\bar{z},\alpha,\beta)$ is not known, we can threat the integrals in Eq. (3) as two unknown complex functions $F_1(\alpha,\beta)$ and $F_2(\alpha,\beta)$:

$$E_{CCD}(\alpha,\beta,t) = e^{-i\omega t}\left[F_1(\alpha,\beta) + e^{2ikz_\psi}F_2(\alpha,\beta)\right]. \tag{4}$$

The field intensity I_{CCD} measured at each pixel of the CCD has the form:

$$I_{CCD}(\alpha,\beta) = \frac{1}{2}c\epsilon_0\; E_{CCD}(\alpha,\beta,t)\cdot E_{CCD}(\alpha,\beta,t)^*, \tag{5}$$

and using the exponential expressions of F_1 and F_2:

$$F_1(\alpha,\beta) = |F_1(\alpha,\beta)|\cdot e^{i\psi_1(\alpha,\beta)}, \tag{6}$$

$$F_2(\alpha,\beta) = |F_2(\alpha,\beta)|\cdot e^{i\psi_2(\alpha,\beta)}, \tag{7}$$

we can rewrite Eq. (5) as:

$$I_{CCD}(\alpha,\beta) = I_{off}(\alpha,\beta) + I_{amp}(\alpha,\beta)\cdot\cos\left[2kz_\psi + \psi(\alpha,\beta)\right], \tag{8}$$

where $I_{off}(\alpha,\beta)$, $I_{amp}(\alpha,\beta)$ and $\psi(\alpha,\beta)$ are real functions:

$$I_{off}(\alpha,\beta) = \frac{1}{2}c\epsilon_0\left[|F_1(\alpha,\beta)|^2 + |F_2(\alpha,\beta)|^2\right], \tag{9}$$

$$I_{amp}(\alpha,\beta) = c\epsilon_0\,|F_1(\alpha,\beta)|\,|F_2(\alpha,\beta)|, \tag{10}$$

$$\psi(\alpha,\beta) = \psi_2(\alpha,\beta) - \psi_1(\alpha,\beta). \tag{11}$$

From Eq. (8) it is seen that the dependency of intensity I_{CCD} on z_ψ at each point on the CCD is described by a cosine function. Its period is equal to $\pi/k = \lambda/2$ which is the same as the periodicity the of illuminating standing wave. I_{CCD} is defined at each point in the CCD plane by three specific parameters I_{off}, I_{amp} and ψ. With the knowledge of these parameters we are able to reconstruct the light intensity patterns $I_{CCD}(\alpha,\beta)$ of the scattered field for any value of z_ψ. How to obtain these parameters is the subject of the next Section.

3. CALIBRATION OF THE INTERFERENCE PATTERNS

By the calibration of the interference patterns we mean here the procedure of determining the parameters $I_{off}(\alpha,\beta)$, $I_{amp}(\alpha,\beta)$ and $\psi(\alpha,\beta)$ at each pixel of CCD camera. Any attempt to predict them theoretically (to find the exact form of impulse response function) would require to involve all the parameters of the setup. They would have to be known with high accuracy or would have to be subjects of some optimization procedures comparing the predictions with the experimental reality. However this is not necessary since we found the way how to determine I_{off}, I_{amp} and ψ parameters experimentally.

Let us have a record of intensity patterns captured while the standing wave illuminating the static particle (scatterer) uniformly moves ($z_\psi = const.\cdot t$). To obtain experimentally such a record is very difficult task because the particles are always fluctuating due to the Brownian motion. To suppress the influence of this thermal motion we have to acquire the record of the intensity patterns in an extremely short time and so we could assume that the particle does not change its position and that its fluctuations are negligible. Therefore one needs an ultra-fast CCD camera and very fast and accurate device to control the position of standing wave via shifting a movable mirror. An example of this record is demonstrated in Fig. 2.

Figure 2. An example of five interference patterns of a polystyrene particle 1.070 μm in diameter illuminated by a standing evanescent wave ($\lambda_{vac} = 532$ nm) taken during fast sweep of the standing wave over the particle by a high-speed CCD camera (IDT X-Stream XS3, 4 GB) with framerate of 6120 fps. Due to the fast movement of the field and the fast recording the particle can be assumed stationary because its fluctuations caused by the Brownian motion or the influence of illuminating field are negligible during the recording period of 0.65 ms. This set of images corresponds to the shift of standing wave equal to one its period (200 nm).

Based on the assumption of uniform movement of the standing wave and the stationarity of the object during the period of recording, $I_{off}(\alpha,\beta)$, $I_{amp}(\alpha,\beta)$, and $\psi(\alpha,\beta)$ can be obtained by fitting the dependency in Eq. (8) to the evolution of recorded intensity at each pixel. An example of the result found by this procedure presents Fig. 3.

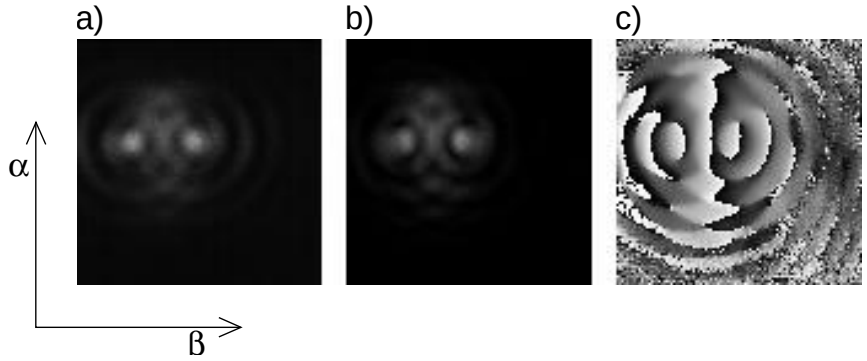

Figure 3. Reconstructed functions: a) $I_{off}(\alpha,\beta)$; b) $I_{amp}(\alpha,\beta)$; c) $\psi(\alpha,\beta)$ (black color corresponds to $-\pi$, white corresponds to π

Now, when I_{off}, I_{amp} and ψ are known, we can reconstruct the intensity pattern I_{CCD} for any value of z_ψ using Eq. (8). In turn comparing the reconstructed patterns with CCD frame of light scattered by the static particle we are now able to determine the position of the standing wave. Since the particle is static, the position of the standing wave z_ψ can be understood here as the relative position of the particle with respect to the standing wave. Therefore when the calibration is done, the comparison of the measured and the reconstructed image reveals the mutual position of the standing wave and the particle even if the particle moves.

4. 2D PARTICLE TRACKING IN THE LATERAL PLANE USING THE STANDING WAVE ILLUMINATION

The lateral plane is understood here as the $\bar{x}\bar{z}$ plane perpendicular to the direction of observation ($\bar{y}$). Once we are able to reconstruct the intensity pattern of scattering particle for any position in the standing wave, we can use such reconstructed patterns for particle tracking in both directions ($\bar{x}$ and $\bar{z}$) perpendicular to the direction of observation ($\bar{y}$). For that case we have to discuss the situation where the free particle moves in the stationary standing wave.

As the particle moves in such static field, the position of the whole intensity pattern of the scattered light imaged on the CCD copies its motion (as in the case of single-beam illumination) but at the same time, the shape of this pattern changes as the particle changes its position with respect to the standing wave (as it was described in the previous Section). To determine the particle positions from the CCD record, we have to find for each frame the right shape of the intensity pattern (using Eq. (8) and I_{off}, I_{amp} and ψ from the callibration procedure) and place it to the right position*. The best way how to shift the reconstructed pattern $I_{CCD}(\alpha, \beta)$ to an arbitrary position (non-integer number of pixels x and z) without adding any noise by resampling of the structure is to use the translational property of the Fourier transform:[35]

$$\begin{aligned} F(A,B) &= FT\left[I_{CCD}(\alpha,\beta)\right], \\ I_{CCD}(\alpha - x, \beta - z) &= IFT\left[F(A,B)e^{-2\pi i(Ax+Bz)}\right], \end{aligned} \tag{12}$$

where FT means the Fourier transform and IFT is the inverse Fourier transform.

One of the options how to decide which is the optimal reconstructed pattern shape and its optimal position is to look for the maximal value of

$$K(x, z, z_\psi) = \sum_{\alpha,\beta} I_{exp}^{\alpha,\beta} \cdot I_{rec}^{\alpha,\beta}(x, z, z_\psi), \tag{13}$$

where $I_{exp}^{\alpha,\beta}$ is the intensity of the examined frame and $I_{rec}^{\alpha,\beta}(x, z, z_\psi)$ is the reconstructed frame for the z_ψ particle position in the standing wave and shifted to the position of x and z.

The output of the optimization process is one value of particle position in the $\bar{x}$ direction (x) and two values for the $\bar{z}$ direction (z and z_ψ).

Obtaining of the z_ψ record (from the pattern shape) is complicated by the fact that due the periodicity of the interference pattern shape we are not able to decide in which period of the field the particle is located. This can be mastered using the CCD camera with such a high framerate that the particle displacement between two adjoining frames is much smaller than the field period. Since we do not evaluate only a single frame but a time record of intensity patterns, the particle position found from one frame is used as the input parameters for the subsequent frame in the process of particle tracking. This assures fast convergence to the correct particle positions. An example of particle position record obtained by the described method is presented in Fig. 4.

It is seen that the above described method provides x and z positions in fractions of pixels but z_ψ values are in micrometers (since we know the wavelength of the illuminating field these data are already calibrated, as follows from Eq. (8)). If the standing wave is stationary, the obtained z and z_ψ positions have to give the same

*This process is restricted to the cases when spherical particles are used (for non-spherical objects the intensity patterns would depend on the object orientation) and when particle fluctuations in the direction of observation (y) are so small that they can not cause any significant changes of observed intensity pattern.

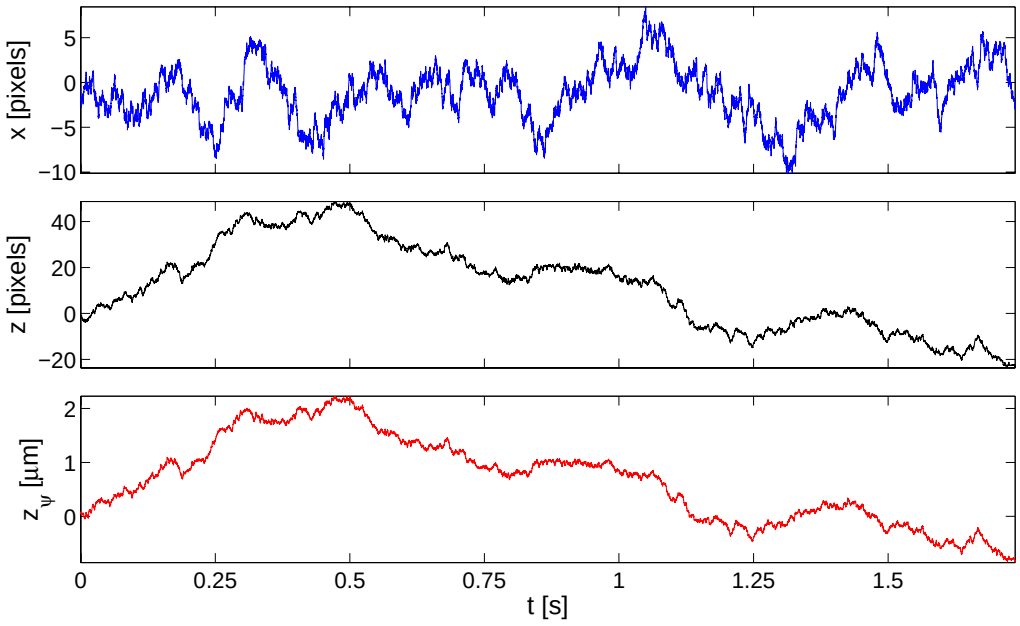

Figure 4. Motion of a particle 1.070 μm in diameter illuminated by a standing evanescent wave ($\lambda_{vac} = 532$ nm). These positions were obtained by the particle tracking method from the CCD record of the same particle as in the case of Fig. 2. The CCD framerate was 6120 Hz and the integration time was set to 2 μs. These particle position data are used in the following explanation to demonstrate all the features of this method.

values. Therefore this property can be used for calibration of z and x data assuming the same properties of the imaging system in both $\bar{x}$ and $\bar{z}$ directions[†]. This procedure of the particle position data calibration is shown in Fig. 5 for the record demonstrated in Fig. 4.

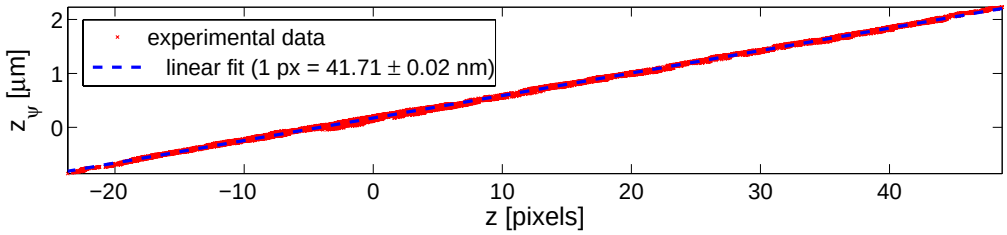

Figure 5. An example of the assignment of the calibration constant between CCD pixels and micrometers. Slope of the linear fit gives the calibration constant.

The difference of z_ψ and calibrated z values $\Delta z = z_\psi - z$ gives us the information about the movement of the standing wave with respect to the imaging system. This brings the possibility to measure the instability of the system. Moreover it opens new possibilities to track the particle even in motional standing wave and to measure precisely their position with respect to the standing wave. The Δz record is presented in Fig. 6 and it

[†]Unfortunately the real experimental setup is not perfectly rigid and there are always some vibrations of the used components which causes a movement of standing wave with respect to the imaging system and the CCD. Since the calibration is performed using all the data points taken over the period of 1.75 s, the influence of these vibrations is suppressed.

designates that the magnitude of the setup instabilities was in tens of nanometers during recording the particle motion presented in Fig. 4.

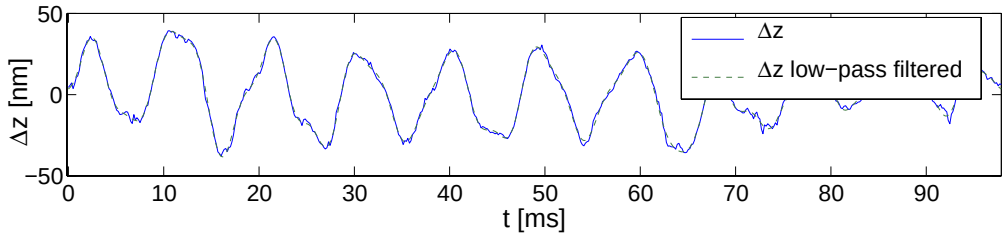

Figure 6. The difference $\Delta z = z_\psi - z$. We can approach the real setup oscillations by filtering out the higher frequencies (≥ 500 Hz). They can be assumed as the noise added by the method inaccuracy.

Δz can also assist to determine the accuracy of the method. The method inaccuracy brings a component of white noise to the Δz record. The magnitude of the white noise can be determined from the spectral analysis of Δz record in the area of high frequencies, where the oscillations of the setup are strongly attenuated. Due to the limited volume of this paper we will not describe this in detail, however for the particle position record presented here (Fig. 4) the inaccuracy of the method (magnitude of the white noise component) is about 1.02 nm. Since the white noise component in Δz is caused by the deviations of both z_ψ and z values and since the x values are obtained the same way as the z values, we can conclude, that the standard deviations caused due to the method inaccuracy do not exceed the limit of 1 nm for all x, z and z_ψ values.

5. PARTICLE TRACKING PERPENDICULARLY TO THE LATERAL PLANE

Particle position detection in the direction of the observation ($\bar{y}$) can be performed if there is some intensity gradient of the illuminating field in this direction. For example in the case of evanescent standing wave the record of y positions can be estimated from the total intensity of the CCD interference patterns. Since there is the exponential intensity decay in the direction perpendicular to the surface where the evanescent field is established by total internal reflection, the y value of particle position can be found as ratio:

$$y = -\log\left(\frac{\sum_{\alpha,\beta} I_{exp}}{\sum_{\alpha,\beta} I_{rec}}\right), \tag{14}$$

where I_{exp} is a CCD image of an interference pattern and I_{rec} is the computed image giving the best pattern match with I_{exp}.

To calibrate these y values we assumed that the velocity distributions of the thermal (Brownian) motion are not influenced by the illuminating field significantly so they are the same for all three axes $\bar{x}$, $\bar{y}$, and $\bar{z}$. Though the distribution of the particle displacements in the period between capturing two adjoining frames (the differences of neighboring positions) has to be the same for all the axes as well. For the calibration constant we use the z_ψ values because they are not influenced by the calibration presented in Fig. 5. Having the difference of neighboring positions $\Delta z_{\psi_j} = z_{\psi_{j+1}} - z_{\psi_j}$ and $\Delta y_j = y_{j+1} - y_j$, the calibration constant is determined as the ratio of mean absolute values of these differences:

$$K(y) = \frac{\sum_{j=1}^{N-1} |\Delta z_{\psi_j}|}{\sum_{j=1}^{N-1} |\Delta y_j|}. \tag{15}$$

The distributions of displacements Δz_{ψ_j} and Δy_j obtained from z_ψ and calibrated y values is shown in Fig. 7.

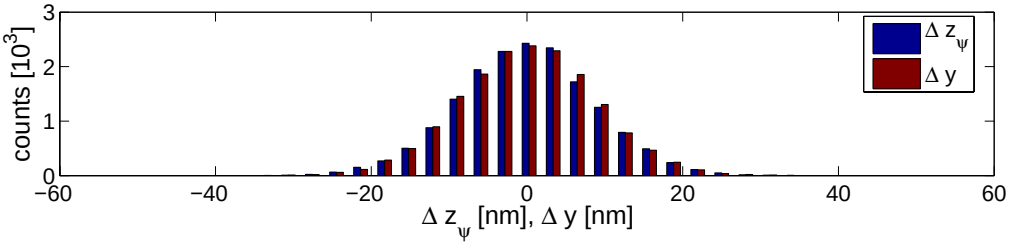

Figure 7. The distributions of differences of neighboring positions Δz_ψ and Δy.

For these y data the zero value is defined by the y position where the particle was placed during the process of interference patterns calibration described in Section 3. Unfortunately we have not found any possibility how to determine this position with respect to the prism which would help us to measure the y data absolutely. The resulting record of y positions is presented in Fig. 8.

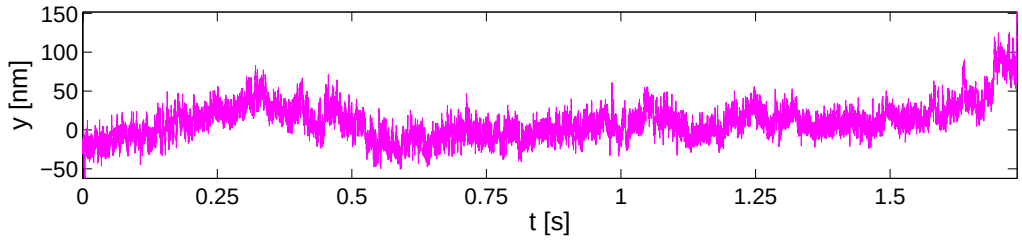

Figure 8. The values of particle positions in the y axis computed from the total intensity ratio done by Eq. (14).

At present we have no opportunity how to estimate the accuracy of the y values. These data are influenced by noise of the CCD camera or the laser power instability and they influence the precision of the data calibration, too. Therefore we use this procedure just as an estimate of the particle behavior along this axis.

6. THE APPLICATIONS OF THE METHOD

Precise tracking of particle position enabled us to determine the properties of standing wave optical traps. Figure 9 shows a histogram of particle positions of a particle with 600 nm in diameter. The particles of this size are very sensitive to the trapping field and therefore some intervals of the standing wave are more frequently occupated than the others. From these histograms we were able to determine the depth (and the stiffness) of the optical traps by fitting the Boltzmann distribution. For all the studied particle sizes the obtained values were in very good agreement with our theoretical predictions based on Lorenz-Mie scattering theory.[34]

Our method of particle tracking is not restricted to the stationary standing wave only. The possibility of particle tracking with respect to the standing wave and at the same time with respect to the laboratory system opens up a prospect to explore in details the particle behavior even in the motional standing wave trap. An example of these possibilities demonstrates Fig. 10. Here we studied the particle behavior in the standing wave movable alternately in a positive or negative direction of the z axis at the uniform velocity. Since the method enabled us to measure the standing wave motion, we could see how often the particle jumps to the neighboring trap site as can be seen in the left column of Fig. 10. At the same time we measured the particle position with respect to the standing wave which gave us the information about the particle behavior inside the trap as it is showen in the right column of Fig. 10. It can be seen that the ability of the particle to follow the movement of the trap, the location of the particle stable position, and the dispersion in particle positions strongly depend on the trap velocity. These experiments together with the theoretical description of these phenomena is currently one of the main streams of our research.

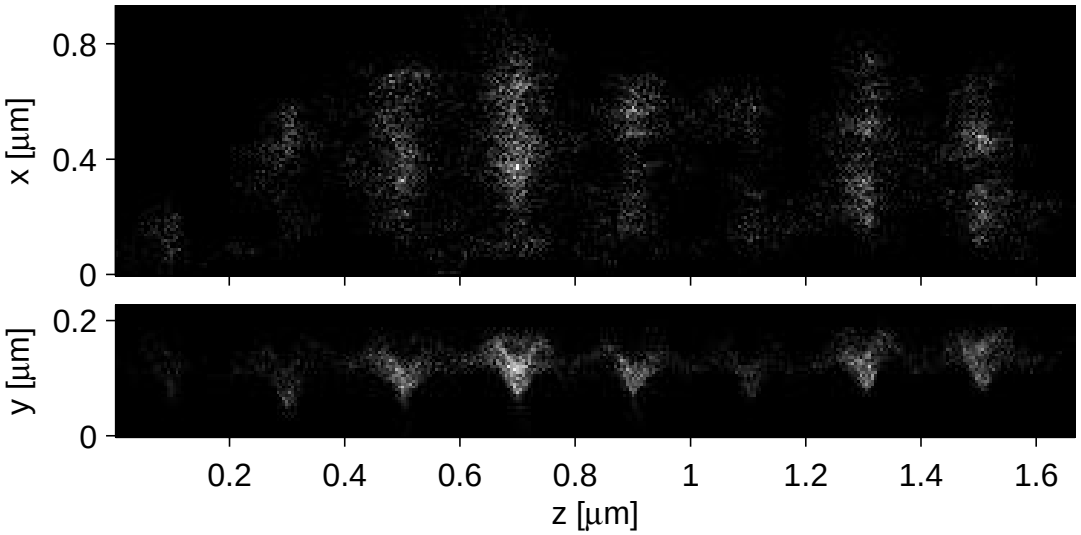

Figure 9. Histograms of particle (diameter 600 nm) positions showing 8 distinct optical traps. Each trap is much narrower in longitudinal direction (z) comparing to the lateral one (x)(see the top image). The bottom image describes how the object behaved in z and y axis. The further one is from the surface (y axis), the wider the spread in the z distribution. The trapping field exponentially decays in this direction and so the object was not so tightly localized.

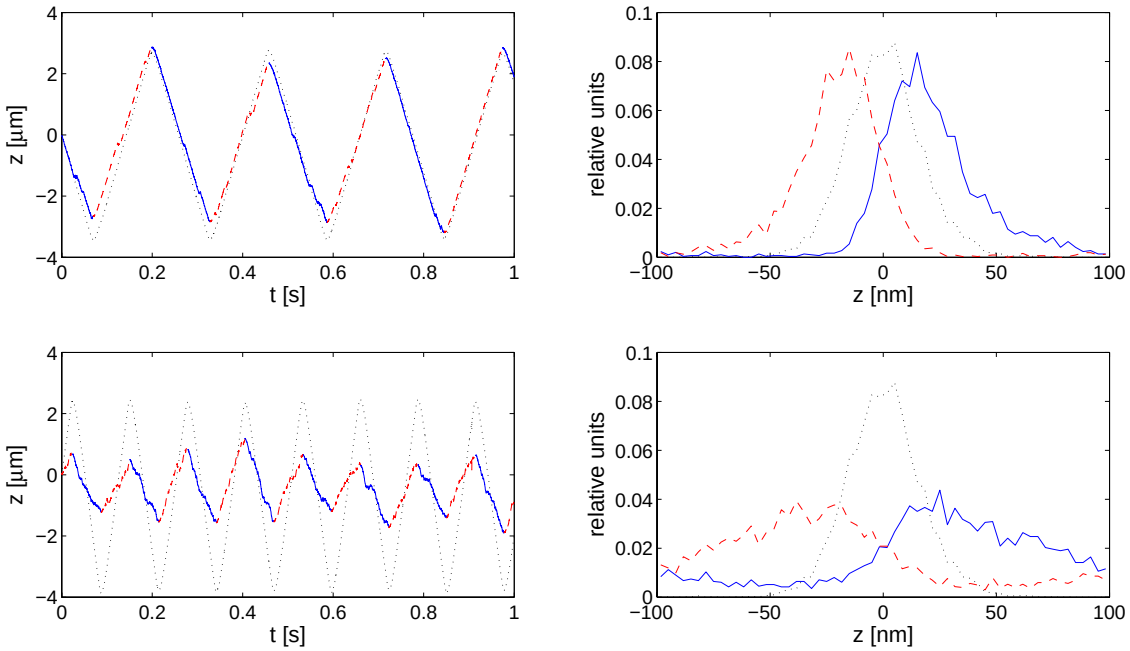

Figure 10. A record of the bead position (left plot column) and histograms of bead center position (right) in slowly (47 μms^{-1}, top raw of plots) and fast (98 μms^{-1}, bottom) moving evanescent standing wave. LEFT: The dashed and the full segments show position of the bead during movement and the dotted line shows the movement of the standing wave. RIGHT: The histograms of particle position with respect to the standing wave. The dashed and full line histograms correspond to the segments of particle movement from the left column, the dotted line is the histogram for particle in unmovable standing wave.

7. CONCLUSIONS

We have presented a new method for the particle tracking by the use of a periodic interference illumination. This illumination can be a standing wave or any kind of two-beams interference field. We have shown some unique features of this method like a self-calibration and setup instability elimination. We have also noticed a 3D-tracking possibility for some kind of illumination fields. Finally we have presented this method applied to the particle tracking in the evanescent standing wave or advanced studies of Brownian dynamics of colloidal particles. This method gave us the most precise results comparing to other available algorithms. The accuracy of this method strongly depends on a CCD camera properties. The bigger frame-rate the camera has, the more precise results this method gives. With the camera used in our experiments we obtained the accuracy in units of manometers.

8. ACKNOWLEDGMENTS

This work was partially supported by the Institutional Research Plan of the Institute of Scientific Instruments (AV0Z20650511), Ministry of Education, Youth, and Sports of the Czech Republic (LC06007), European Commission via 6FP NEST ADVENTURE Activity (ATOM3D, project No. 508952), and the Grant Agency of the Academy of Sciences (IAA1065203).

REFERENCES

1. K. Svoboda, C. F. Schmidt, B. J. Schnapp, and S. M. Block, "Direct observation of kinesin stepping by optical trapping interferometry," *Nature* **365**, pp. 721–727, 1993.
2. J. T. Finer, R. M. Simmons, and J. A. Spudich, "Single myosin molecule mechanics: piconewton forces and nanometric steps," *Nature* **368**, pp. 113–119, 1994.
3. G. J. L. Wuite, S. B. Smith, M. Young, D. Keller, and C. Bustamante, "Single-molecule studies of the effect of template tension on T7 DNA polymerase activity," *Nature* **404**, pp. 103–106, 2000.
4. D. E. Smith, S. J. Tanse, S. B. Smith, S. Grimes, D. L. Anderson, and C. Bustamante, "The bacteriophage ϕ29 portal motor can package DNA against a large internal force," *Nature* **413**, pp. 748–752, 2001.
5. M. J. Lang, P. M. Fordyce, and S. M. Block, "Combined optical trapping and single molecule fluorescence," *J. Biol.* **2**, pp. 2–6, 2003.
6. A. D. Mehta, M. Rief, J. A. Spudich, D. A. Smith, and R. M. Simmons, "Single-molecule biomechanics with optical methods," *Science* **283**, pp. 1689–1695, 1999.
7. C. Bustamante, Z. Bryant, and S. B. Smith, "Ten years of tension: single-molecule dna mechanics," *Nature* **421**, pp. 423–427, 2003.
8. J. C. Crocker and D. G. Grier, "Methods of digital video microscopy for colloidal studies," *J. Colloid Interface Sci.* **179**, pp. 298–310, 1996.
9. P. T. Korda, G. C. Spalding, and D. G. Grier, "Evolution of a colloidal critical state in an optical pinning potential landscape," *Phys. Rev. B* **66**, p. 024504, 2002.
10. K. Ladavac, K. Kasza, and D. G. Grier, "Sorting mesoscopic objects with periodic potential landscapes: Optical fractionation," *Phys. Rev. E* **70**, p. 010901, 2004.
11. M. P. MacDonald, G. C. Spalding, and K. Dholakia, "Microfluidic sorting in an optical lattice," *Nature* **426**, pp. 421–424, 2003.
12. L. P. Faucheux, L. S. Bourdieu, P. D. Kaplan, and A. J. Libchaber, "Optical thermal ratchet," *Phys. Rev. Lett.* **74**, pp. 1504–1507, 1995.
13. S.-H. Lee and D. G. Grier, "One-dimensional thermal ratchets," *J. Phys.: Condens. Matter* **17**, pp. S3685–S3695, 2005.
14. L. Novotny, M. R. Beversluis, K. S. Youngworth, and T. G. Brown, "Longitudinal field modes probed by single molecules," *Phys. Rev. Lett.* **86**, pp. 5251–5254, 2001.
15. M. K. Cheezum, W. F. Walker, and W. H. Guilford, "Quantitative comparison of algorithms for tracking single fluorescent particles," *Biophysical Journal* **81**, p. 23782388, 2001.
16. R. E. Thompson, D. R. Larson, and W. W. Webb, "Precise nanometer localization analysis for individual fluorescent probes," *Biophys. J.* **82**, pp. 2775–2783, 2002.

17. M. Speidel, A. Jonáš, and E.-L. Florin, "Three-dimensional tracking of fluorescent nanoparticles with sub-nanometer precision by use of off-focus imaging," *Opt. Lett.* **28**(2), pp. 69–71, 2003.
18. M. Wu, J. W. Robrts, and M. Buckley, "Three-dimensional fluorescent particle tracking at micron-scale using a single camera," *Exp. Fluids* **38**, pp. 461–465, 2005.
19. I. M. Peters, B. G. de Grooth, J. M. Schins, C. G. Figdor, and J. Greve, "Three-dimensional single-particle tracking with nanometer resolution," *Rev. Sci. Instrum.* **69**, pp. 2762–2766, 1998.
20. I. M. Peters, Y. van Kooyk, S. J. van Vliet, B. G. de Grooth, C. G. Figdor, and J. Greve, "3D single-particle tracking and optical trap measurements on adhesion proteins," *Cytometry* **36**, pp. 189–194, 1999.
21. M. W. Allersma, F. Gittes, M. J. deCastro, R. J. Stewart, and C. F. Schmidt, "Two-dimensional tracking of ncd motility by back focal plane interferometry," *Biophys. J.* **74**, pp. 1074–1085, 1998.
22. F. Gittes and C. F. Schmidt, "Interference model for back-focal plane displacement detection in optical tweezers," *Optics Letters* **23**, pp. 7–9, 1998.
23. A. Pralle, M. Prummer, E.-L. Florin, E. H. K. Stelzer, and J. K. H. Horber, "Three-dimensional high-resolution particle tracking for optical tweezers by forward scattered light.," *Micr. Res. Techn.* **44**, pp. 378–386, 1999.
24. A. Rohrbach and E. H. K. Stelzer, "Three-dimensional position detection of optically trapped dielectric particles," *J. Appl. Phys.* **91**, pp. 5474–5488, 2002.
25. M.-T. Wei and A. Chiou, "Three-dimensional tracking of brownian motion of a particle trapped in optical tweezers with a pair of orthogonal tracking beams and the determination of the associated optical force constants," *Opt. Express* **13**, pp. 5798–5806, 2005.
26. W. Denk and W. W. Webb, "Optical measurment of picometer displacements of transparent microscopics objects," *Appl. Opt.* **29**, p. 2382, 1990.
27. B. Sick, B. Hecht, and L. Novotny, "Orientational imaging of single molecules by annular illumination," *Phys. Rev. Lett.* **85**, pp. 4482–4485, 2000.
28. R. J. Oetama and J. Y. Walz, "Translation of colloidal particles next to a flat plate using evanescent waves," *Coll. and Surf. A* **211**, pp. 179–195, 2002.
29. R. J. Oetama and J. Y. Walz, "A new approach for analyzing particle motion near an interface using total internal reflection microscopy," *J. Colloid Interface Sci.* **284**, pp. 323–331, 2005.
30. A. R. Clapp, A. G. Ruta, and R. B. Dickinson, "Three-dimensional optical trapping and evanescent wave light scattering for direct measurement of long range forces between a colloidal particle and a surface.," *Rev. Sci. Instrum.* **70**, pp. 2627–2636, 1999.
31. A. R. Clapp and R. B. Dickinson, "Direct measurement of static and dynamic forces between a colloidal particle and a flat surface using a single-beam gradient optical trap and evanescent wave light scattering," *Langmuir* **17**, pp. 2182–2191, 2001.
32. T. Čižmár, V. Garcés-Chávez, K. Dholakia, and P. Zemánek, "Optical conveyor belt for delivery of submicron objects," *Appl. Phys. Lett.* **86**, pp. 174101–1–174101–3, 2005.
33. M. Šiler, T. Čižmár, M. Šerý, and P. Zemánek, "Optical forces generated by evanescent standing waves and their usage for sub-micron particle delivery," *Appl. Phys. B* **84**, pp. 157–165, 2006.
34. T. Čižmár, M. Šiler, M. Šerý, P. Zemánek, V. Garcés-Chávez, and K. Dholakia, "Optical sorting and detection of sub-micron objects in a motional standing wave," *Phys. Rev. B* , to be published.
35. R. C. Gonzalez and P. Wintz, *Digital Image Processing*, Addison-Wesley Publishing Company, Reading, 1987.